ELSEVIER

Journal of Chromatography A, 707 (1995) 45–55

JOURNAL OF CHROMATOGRAPHY A

Nuclear magnetic resonance and the design of chromatographic separations

E.N. Lightfoot*, A.M. Athalye, J.L. Coffman, D.K. Roper, T.W. Root

Department of Chemical Engineering, University of Wisconsin, Madison, WI 53706, USA

Abstract

The design of commercial chromatographic separations is an increasingly important subject as the number of products being introduced to the market and pressures for cost containment continue to increase. Of particular concern are the development of more productive columns, dealing with the large number of design parameters of industrial importance and increasing the scale of production. It is therefore important to relate macroscopic column performance to underlying physico-chemical fundamentals, and important among these are mass transfer and fluid mechanics. It is shown here that well established nuclear magnetic resonance techniques can be helpful in characterizing the diffusion and flow behavior of commercial columns and for obtaining the insights needed to develop new designs. It is also suggested that the design parameters so obtained be incorporated into a non-dispersive formulation for describing column behavior.

1. Introduction

Much of the chromatographic literature derives from experience with differential chromatography, in which small mixed feed pulses are separated by differential migration of solutes down a long column. Moreover, most present-day columns are constructed as granular beds of near-spherical adsorbent beads within which Fick's second law of diffusion adequately expresses solute transport. This emphasis has led to simple expressions for separation efficiency based on a dispersion-dominated model and a Gaussian distribution for each solute within the column. The shapes of these distributions are defined simply by a mean solute migration rate and a global measure of column performance known as the number of equivalent theoretical plates, and this is often sufficient for data correlation.

Simple plate models also appear to be useful for predicting the course of protein separations in commercial columns in terms of separately determined parameters such as diffusion coefficients in the moving and adsorbent phases, adsorption rate constants and convective dispersion coefficients. This is suggested, for example, in Fig. 1 [1], where a comparison of observed plate heights with a priori prediction from separately measured contributing parameters is shown for a commercial packing as a function of solvent percolation velocity. Agreement between observation and prediction is excellent, and the individual contributions to plate height are simply additive as required by accepted theory [14]. The dominance of convective dispersion and internal diffusional resistance shown here is common.

* Corresponding author.

0021-9673/95/$09.50
SSDI 0021-9673(95)00077-1

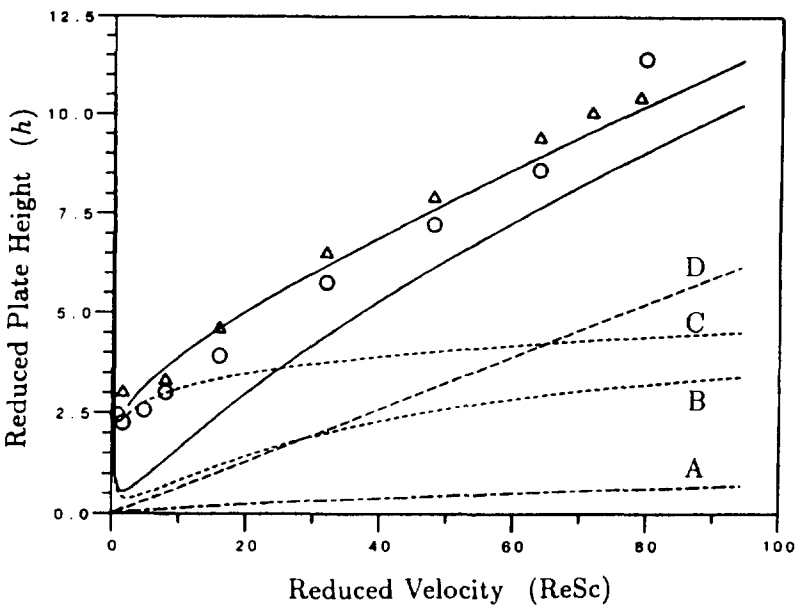

Fig. 1. Predictability of plate heights. Plate height data compared with a priori prediction for an 11.5 × 25 cm I.D. glass column packed with Toyopearl HW65C. Elution of 0.1-ml bovine hemoglobin samples with concentrations of (○) 10, (△) 50 and (□) 100 mg/ml. The predicted results are calculated as follows: (A) mobile phase transfer from Ref. [1]; (B) axial dispersion using Gunn's correlation (see Ref. [1]); (C) axial dispersion using the correlation of Miller and King (see Ref. [1]); (D) intraparticle diffusion using data of Gibbs et al. [26]. The lower and upper solid lines represent total reduced plate height using curves B and C, respectively. Reproduced with permission from [1].

There have, however, been surprisingly few quantitative tests of such models, and careful analysis of these predictions shows that the assumptions leading to the assumed concentration profiles are barely valid in many cases of practical interest. Moreover, the pulsed field gradient method of estimating diffusivity has yet to be thoroughly validated, and there is considerable uncertainty as to the magnitudes of convective dispersion. It would therefore be highly desirable to carry out an extensive systematic investigation of model validity.

There is in addition an increasing interest in using higher solute concentrations, operating in more complex modes and using radically different column designs. Gradient elution techniques are becoming more important [2–4], there is increasing discussion of simulated moving bed counterflow [5,6] and electrophoretic and other new mass transfer mechanisms are being seriously considered. Displacement chromatography [7] continues to be of interest, and new chemical systems are being developed to make it more attractive. New packing and column geometries are also appearing, for example, perfusive beads [8], fluidized beds and membrane columns [9,10]. Still more radical designs, for example, bundles of hollow fibers with adsorptive coatings on their walls, may be just over the horizon. Dealing effectively with these developments will require both effective strategies and more powerful modeling techniques to implement them. More effective data acquisition techniques are also needed.

Modeling effectiveness and economy will become increasingly important, to speed planning and data acquisition in the extensive experimental program needed to produce an acceptable and commercially viable process. It will be necessary to speed experimental programs as much as possible and to predict the behavior of commercial columns from small amounts of laboratory data. Existing dispersive models developed for long columns and low loadings

simply are not adequate for this purpose, and suggestions will be made below for replacing them.

Most important of all is the adequate characterization of column performance. Data needed include diffusion coefficients, adsorptive rate constants and, often neglected, detailed descriptions of flow behavior: the assumption of uniform one-dimensional flow is by no means always adequate. Suggestions will be made for economic and powerful means for obtaining such data, with emphasis on nuclear magnetic resonance techniques.

2. Basic theory

The concept of theoretical plates goes back to the 1941 paper of Martin and Synge [11] and was critically reviewed by van Deemter et al. in 1956 [12] and again by Karol in 1989 [13]. It may be simply expressed for differential chromatography in the form

$$c_i(z,t) = c_0 \cdot \frac{e^{-(N-2)[(z-z_0)/H]^2}}{\sqrt{2\pi N}} \tag{1}$$

where c_i is the local fluid phase solute concentration at any position z and time t, c_0 is a normalization constant and

$$N \equiv z_0/H \tag{2}$$

is the number of "plates" in a length z_0 of the column. This length z_0 in turn is the position of the peak solute concentration defined by

$$z_{0,i} = vt/(1+k_i) \tag{3}$$

where

$$k_i = \frac{\bar{t}_i - \bar{t}_0}{\bar{t}_0} \tag{4}$$

$\bar{t}_i$ and $\bar{t}_0$ being the mean residence times of species i and the carrier solvent, species 0, respectively, and v is the interstitial solvent velocity. For many practical purposes z_0 may be taken to be the length of the column, L. The normalization constant c_0 is the initial fluid concentration in the first plate if the initial solute mass m_0 is distributed uniformly and at equilibrium over this plate:

$$c_0 \equiv m_0/[(1+k_i)A\varepsilon_b H] \tag{5}$$

where A is the column cross-sectional area, ε_b is the volume fraction of column occupied by fluid and m_0 is the mass of solute fed. In practice, the solute profiles at large z_0/H are not very sensitive to the initial solute distribution just so long as it is "reasonably" sharp.

Historically, this distribution was obtained from a model of N mixing tanks in series and approximating the resulting Poisson distribution by a Gaussian with the same mean and variance. The correspondence between these two distributions is only good near the solute peak for a "large" number of plates, and never at large distances from the peak. It is in any event far preferable to work from a reliable differential description, and that most commonly used [14] is

$$\frac{\partial c_i}{\partial t} + v \cdot \frac{\partial c_i}{\partial z} - E \cdot \frac{\partial^2 c_i}{\partial z^2} = -\left(\frac{1-\varepsilon_b}{\varepsilon_b}\right)\frac{\partial c_{ib}}{\partial t} \tag{6}$$

with

$$\frac{\partial c_{ib}}{\partial t} = \frac{3K_c}{R}(c_i - \alpha c_{ib}) \tag{7}$$

where E is an effective axial diffusion coefficient to allow both for true diffusion and the effects of non-uniform flow (convective dispersion), c_{ib} is concentration of solute i in the stationary or bead phase, which is assumed to consist of uniform spheres with radius R, and K_c is an overall mass transfer coefficient to allow for boundary-layer diffusional resistance, intra-particle diffusion and slow adsorption on the inner surfaces of the adsorbent [14,1]. The distribution coefficient is

$$\alpha = c_i^*/c_{ib} \tag{8}$$

where the asterisk denotes an equilibrium value.

The Fickian or axial diffusive term containing the effective diffusion coefficient E is an approximation based on a mixing model not far different from that on which the plate model depends, but it is essentially species independent and local. It appears to introduce little error into the integral description (Eq. 1), but the implied diffusion

behavior does not actually exist. For example, no solute is transported upstream as required in principle by this term. It is used primarily to obtain the mathematically convenient integral description of Eq. 1. The mass transfer coefficient also contains a lumped parameter approximation which goes back to Glueckauf and Coates [15]. It was shown to be a suitable first approximation for then existing long columns by Reis et al. [17].

Use of an axial dispersion term does produce some problems in specifying boundary conditions, and it is customary to get around these by using "long-column" boundary conditions:

$$\text{as } z \Rightarrow \pm\infty,\ c,\ \partial c/\partial z \Rightarrow 0 \tag{9}$$

with the normalizing condition

$$\varepsilon_b A \int_{-\infty}^{\infty} \left[1 + \frac{(1-\varepsilon_b)}{\alpha\varepsilon_b}\right] c\, dz = m_0 \tag{10}$$

A complete solution of Eqs. 6–10 is extremely cumbersome [21], but a number of convenient close approximations are available. The most widely used is based on the assumption, first formulated by Klinkenberg and Sjenitzer [16], that all contributions to the variance of the exit distribution are additive, and it leads to the very compact expression

$$H = \frac{2E}{v} + \frac{2}{3}\cdot\frac{Rv}{\alpha K_c}\cdot\frac{k}{(1+k)^2} \tag{11}$$

The work of Reis et al. [17] is of particular interest, in showing that Eq. 1 with plate height given by Eq. 11 does represent a correct first-order approximation which was accurate enough for almost all columns in use at that time. Eq. 11 can also be used to define equivalent total dispersion coefficients E_{eff} or mass transfer coefficients K_{eff} by

$$H \equiv \frac{2E_{eff}}{v} \equiv \frac{2}{3}\cdot\frac{Rv}{\alpha K_{eff}}\cdot\frac{k}{(1+k)^2} \tag{12}$$

Eq. 12 permits the elimination of either the dispersion term or the mass transfer term in Eqs. 6 and 7 and yields two widely used approximations, as follows.

2.1. Dispersion model

Here one assumes equilibrium between the fluid and bead phases and uses an effective dispersion coefficient as given by Eq. 12 to compensate for this omission:

$$(1+k_i)\frac{\partial c_i}{\partial t} = \frac{Hv}{2}\cdot\frac{\partial^2 c_i}{\partial z^2} - v\cdot\frac{\partial c_i}{\partial z} \tag{13}$$

where the identity

$$\left[\frac{\alpha_i\varepsilon_b + (1-\varepsilon_b)}{\alpha_i\varepsilon_b}\right] = (1+k_i) \tag{14}$$

has been used. For long columns Eqs. 13 and 14 thus reduce to Eq. 1 (Ref. [19], Sect. 10.3). This simplicity is the basis of popularity for the dispersion model.

2.2. Mass-transfer model

Now one neglects dispersion in the direction of flow but uses a smaller interphase mass transfer coefficient to compensate for this omission:

$$\frac{\partial c_i}{\partial t} + v\cdot\frac{\partial c_i}{\partial z} = -\left(\frac{1-\varepsilon_b}{\varepsilon_b}\right)\frac{\partial c_{ib}}{\partial t} \tag{15}$$

with

$$\frac{\partial c_{ib}}{\partial t} = \frac{2v}{\alpha H}\cdot\frac{k}{(1+k)^2}(c_i - \alpha c_{ib}) \tag{16}$$

2.3. Comparison

Eqs. 13–16 are very different in appearance, and so are their integrated forms. Thus for batch adsorption, where the boundary conditions are

at $z = 0$, $y \equiv c_i/c_{feed} = 1$ for $t > 0$;

at $t = 0$, $c = 0$ for $z > 0$,

the corresponding profiles are

$$y \equiv c_i/c_{feed} = \frac{1}{2}\left[1 + \text{erf}\left(\frac{\frac{z}{z_0} - 1}{\sqrt{N/2}}\right)\right] \text{ (dispersion model)} \tag{17}$$

$$y = J(\zeta, \tau) \text{ (mass transfer model)} \tag{18}$$

where Brinkley's J-function [20] is given by

$$J(u) = 1 - \int_0^u \exp[-(\tau + u')] \cdot J_0[i(4\tau u')^{3/2}]\, du' \tag{19}$$

and

$$\zeta \equiv z\left(\frac{K_{eff}}{Rv}\right)\left[\frac{3(1-\varepsilon)}{\varepsilon}\right] \quad \tau \equiv \left(\frac{3K_{eff}}{\alpha R}\right)(t - z/v)$$

Numerical comparison [18] shows the two distributions to be nearly identical for most situations of interest: there is very little model sensitivity. The mass-transfer model is not convenient for analytical description, but it is probably the better suited to numerical computation. Even in the case of membrane chromatographs axial diffusion is negligible under most circumstances [22], and one can simply march ahead from the inlet.

However, plate heights are in general species dependent, particularly when dealing with species of appreciably different properties, for example, proteins and eluting solvents. Moreover, many systems show both thermodynamic and diffusional interactions between solutes to be separated. Thermodynamic interactions can easily be dealt with using the mass transfer model by writing a matrix set of equations in which the α_i are functions of all solute concentrations. Diffusional interactions must at present be ignored, for lack of data (see, however, refs. [23] and [24]). Finally, we note that describing intra-particle processes by a simple lumped-parameter mass-transfer coefficient may not be permissible at the very high percolation velocities used in some present processes.

3. Experimental

There have to date been surprisingly few data suitable for testing the above models, particularly for the chromatographic separation of proteins. This is true even for thermodynamics at high protein concentration, but it is particularly true for transport characteristics. This is our primary concern here, and we review some recent results obtained by nuclear magnetic resonance techniques. Details are provided in the references given.

3.1. Diffusion coefficients

Diffusion of proteins within the "pores" of chromatographic adsorbents is complicated by the essentially multi-component nature of protein diffusion, interaction of proteins with the adsorbent and the rapid response of currently available adsorbent particles to composition changes at their surfaces. Pseudo-binary approximations appear to be reasonable [25], although some ambiguities in data interpretation remain. We return to the problem of protein–pore interactions shortly. Rapid response times preclude obtaining differential diffusion coefficients by the classical step or pulse response techniques, and the opacity of most adsorbents also eliminates optical techniques as well.

Our research group has therefore pioneered the use of magnetic labeling, or pulse field gradient nuclear magnetic resonance (PFGNMR), techniques and have shown that one can obtain reliable measures of mutual diffusion coefficients by this approach [26], from very dilute solutions up to 20% or more protein by mass. Initial results for size-exclusion media gave what appear to be the most accurate data available, and it was these data which permitted the test of the plate model shown in Fig. 1. It should be noted that the PFGNMR technique provides tracer diffusion coefficients, and thermodynamic correction terms must be used to determine the desired mutual diffusivities, except in the limiting case of dilute solutions. Moreover, in work published to date it was necessary to add fluorine labels to the proteins.

We have now begun a systematic study of protein–pore interactions, and the preliminary data in Fig. 2 [27] show reasonably good agreement with available hindred diffusion theory [29]. Shown in Fig. 2 are the effect of the ratio of protein Stokes radius r_s to pore radius, R_{pore}, on protein diffusivity. The ordinate is the ratio of pore diffusivity, as determined by PFGNMR, to

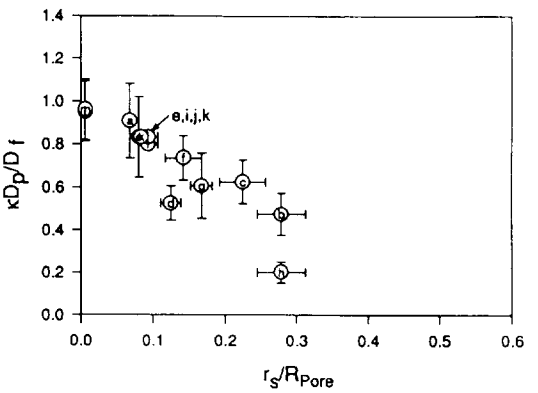

Fig. 2. Intraparticle diffusion coefficients by PFGNMR. Shown are the intraparticle diffusion coefficients for several proteins in various chromatographic media, plotted verses the ratio of protein Stokes radius r_s and pore size R_p. The intraparticle diffusion coefficients D_p are scaled by the diffusion coefficients in free solution D_f and by a tortuosity factor κ of 2, as described in the text. BP300 and BP500 Baker bonded-phase silica, 300 and 500 Å, respectively. TSK-HW65, TSK-HW55 and TSK-HW650S-Phenyl from TosoHaas. Sepharose Fast Flow, Sepharose High Performance and Source from Pharmacia. FOva and FCon = fluorine-labeled ovalbumin and conalbumin, respectively; Lys = hen egg-white lysozyme. Pore sizes for Sepharose and HW55 were estimated from exclusion data. Correlations for data discussed elsewhere. (a) Ova/HW65; (b) FOva/HW55; (c) Ova/HW55; (d) FOva/Source; (e) Fcon/HW65; (f) Lys/BP300; (g) FOva/BP500; (h) FOva/BP300; (i) FOva/Sepharose FF; (j) FOva/Sepharose HP; (k) FOva/HW65S Phenyl; (l,m) HOH/BP300, HW65.

free solution diffusivity multiplied by tortuosity κ. The tortuosity was estimated as 2.0 from the analysis of Epstein [28], and this agrees reasonably well with the value of 2.2 ± 0.4 found experimentally by Gibbs et al. [26] for a large-pore size-exclusion particle. The diffusivity ratios are essentially independent of protein concentration under the conditions used.

Data are shown in Fig. 2 for both fluorine-labeled and unlabeled proteins, with the latter measurements obtained from proton PFGNMR. The proton NMR data were obtained by utilizing the time-scale separation of label decay for water, protein and adsorbent matrix. These are only reliable for moderately concentrated proteins, but labeling had no discernible effect on diffusivity.

3.2. Fluid mechanic considerations

Magnetic resonance techniques are also proving useful for studying the fluid mechanics of chromatographic operations, through both static and flow magnetic resonance imaging. Here we consider the distortions resulting from the high viscosity of concentrated protein solutions and the effects of mechanical design in a stacked-membrane chromatograph as examples.

High loading and fingering

Fig. 3 shows a magnetic resonance image of two protein bands migrating down a column of 1 in. I.D. (see [30]). Here flow is from top to bottom as shown, and the image is of a plane containing the column axis. The protein is hemoglobin at a feed concentration of 100 mg/ml in the lower band and 70 mg/ml in the second. The flow-rate was 0.1 ml/min and the eluting buffer was 0.1 *M* sodium citrate (pH 6.0). The packing was 75-μm diameter ToyoPearl HW40C beads, which completely excluded the hemoglobin, and the column was as packed by the manufacturer (TosoHaas). The protein is labeled with Gd attached using diethylenetriamine (Aldrich) to provide contrast. The photograph is produced from a three-dimensional image taken in a General Electric 1.5 T whole-body imager in the University of Wisconsin medical school, and

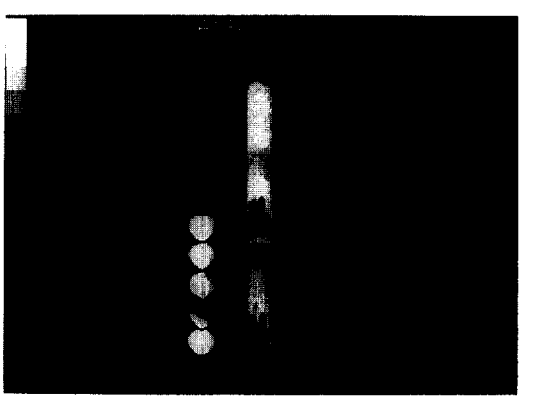

Fig. 3. "Fingering" of protein bands under non-adsorbing conditions. Experimental details are described in the text. Flow is downward as shown.

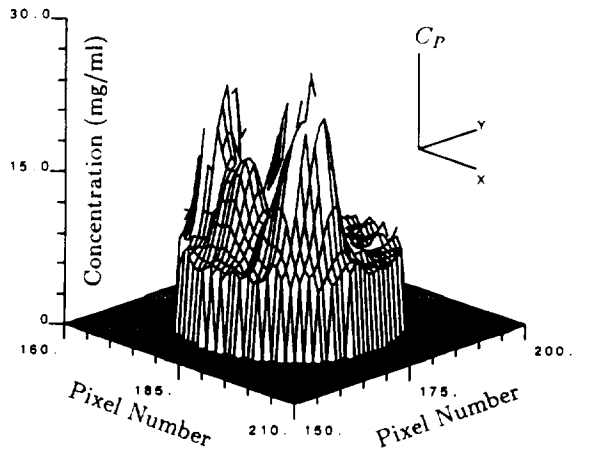

Fig. 4. Concentration profile of an eroded front. Shown are calculated protein concentrations over a cross-sectional slice through the upper region of the central band of Fig. 3. Severe non-uniformities are evident, in agreement with the severe distortion seen in Fig. 3.

calibrating experiments permit construction of protein concentration profiles. Examples for the upstream and downstream regions of the upper protein band are shown in Figs. 4 and 5, respectively.

Both protein bands are seen to be unstable and badly eroded at their trailing edges, whereas the leading edges are relatively sharp. The cause of the erosion is hydrodynamic instability resulting from the higher viscosity of the protein solution relative to the buffer. The situation is basically similar to that occurring in the secondary recovery of oil from petroleum-bearing rock. Comparison of our results with those obtained by Yamomoto et al. [31], who sliced columns and examined the protein distribution in the slices visually, show that the onset of fingering is very sensitive to experimental detail, but in both cases variance of the exit concentration distributions increased strongly with increasing feed protein concentration.

Flow characterization of a stacked-membrane chromatograph

Here we examine the performance of a stacked-membrane chromatograph, the MemSep 1000 manufactured by Millipore and shown schematically in Fig. 6. This device consists essentially of 40 microporous membranes compressed into a cylindrical shape about 17.17 mm I.D. by 5 mm high. The stack is sealed by annular gaskets at its periphery as indicated.

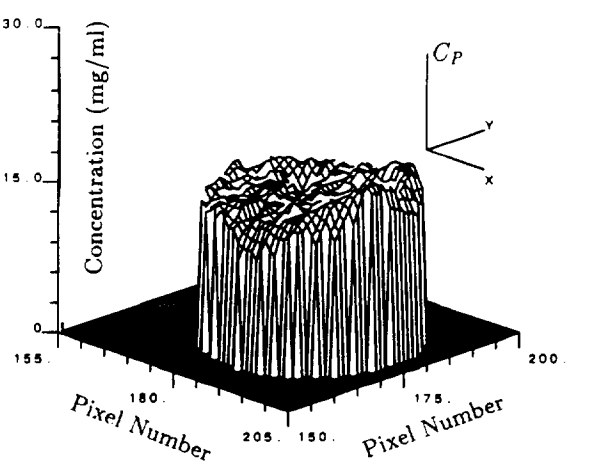

Fig. 5. Concentration profile of a stable front. Calculated protein concentrations over a cross-section near the lower edge of the central band of Fig. 3. Note that this distribution is relatively uniform.

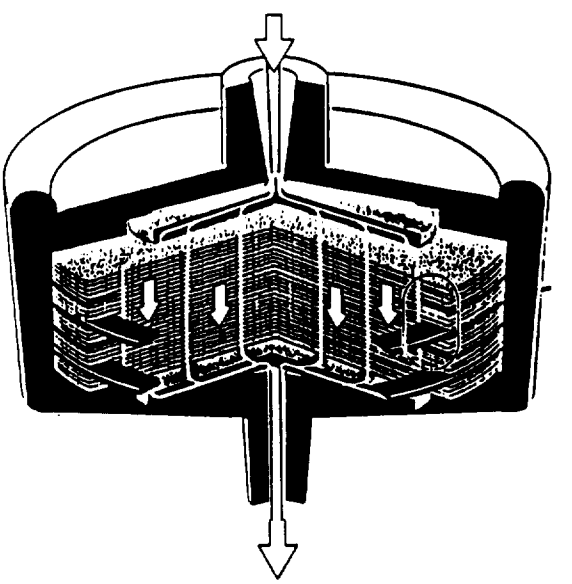

Fig. 6. Schematic view of the stacked membrane cartridge, MemSep, as designed by Millipore.

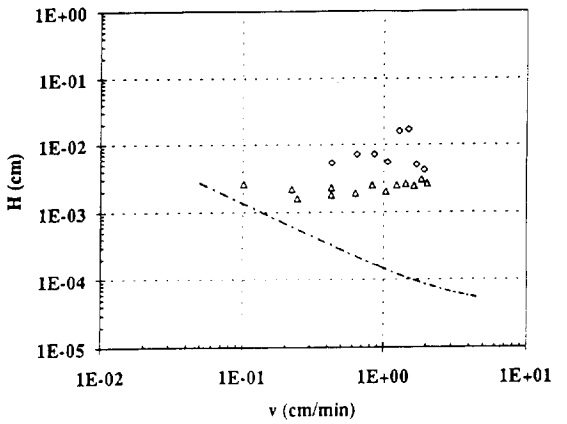

Fig. 7. Experimental stacked-membrane plate heights. The points represent data reported by Raths [35] (◇) and by Gerstner [10] (△). The dotted line represents the expectation from calculations of 2D convective dispersion [32].

Preliminary analysis (see [32]) suggests that such a device should have a very small plate height, on the order of 1 μm, which should actually decrease with increase in flow-rate.

However, the actual performance is much poorer. Thus, it may be seen in Fig. 7 that reported values are in the range 20–80 μm. Fig. 8 shows that the response to a pulse input under non-adsorbing conditions is badly skewed, with pronounced tailing. Both of these results suggest major maldistribution of flow. Moreover, calculations of plate height by Yamomoto [33] obtained under conditions of self-sharpening fronts show much higher plate heights than those obtained under linear conditions. This discrepancy is probably due to the assumption of flat velocity profiles: macroscopically non-uniform flow would give plate heights increasing in proportion to column length.

Both fluid mechanic analysis [34,35] and magnetic resonance imaging bear out the suggestion of maldistribution, and here we concentrate on the imaging work. Figs. 9 and 10 show the internal structure of a MemSep, at zero flow in

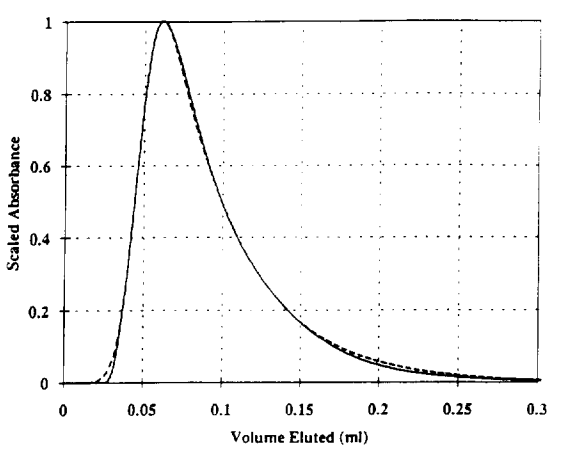

Fig. 8. Pulse response of a MemSep cartridge. Residence-time density from an assembly consisting of precolumn tubing, fittings, injection valves and a MemSep 1000 cartridge (solid line) compared with a best fit using an exponentially modified Gaussian distribution [36].

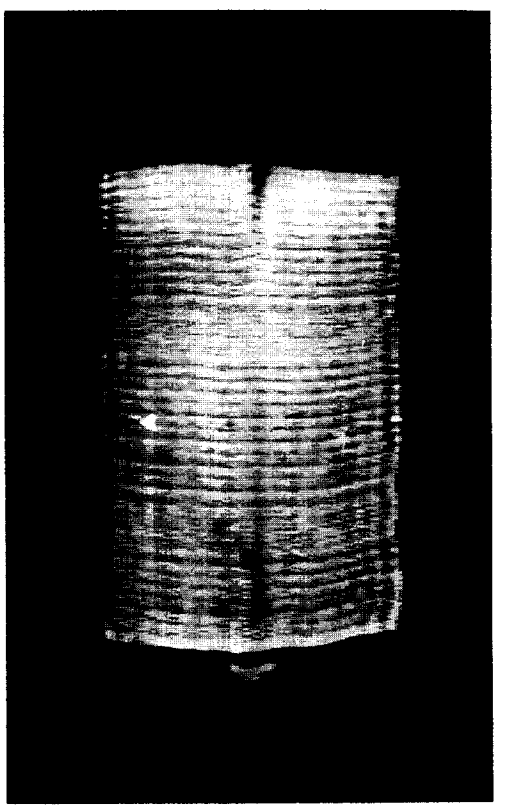

Fig. 9. Static NMR image in a MemSep cartridge under no-flow conditions. Shown is a view of a 1-mm planar slice containing the apparatus axis for the MemSep 1000. Brightness is approximately proportional to proton density. From Roper [32].

Fig. 9 and at 10 ml/min buffer flow in Fig. 10. Individual membranes, approximately 125 μm thick, are seen clearly, as are the compressed membranes between the annular gaskets. The spatial resolution is therefore of the order of 50 μm. The space between the gaskets represents a large reservoir of fluid with poor diffusional access to the flowing buffer, and it undoubtedly contributes significantly to tailing. However, there is clear evidence of significant distortion under flow conditions, with "sagging" of the membranes and the opening up of a dead space at the upstream end of the device. Both of these effects are likely to result in macroscopic maldistribution of flow and although the flow-rate represented in Fig. 10 is higher than that recommended by the manufacturer, similar distortion occurs at lower flow-rates.

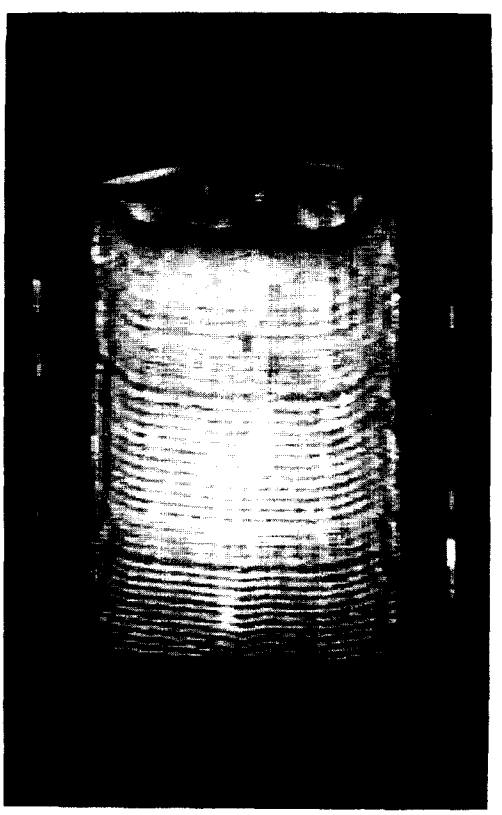

Fig. 10. Static NMR image under flow conditions. Shown is the same view as in Fig. 9, but with water flowing through the cartridge at a rate of 10 ml/min. This flow creates a back pressure of 46 p.s.i., which distorts both the cartridge casing and the membrane stack itself. From Roper [32].

Direct evidence of non-uniform flow is shown in Fig. 11, which describes the velocity distribution over a cross-sectional area of the Memsep. It can be seen that the velocity drops significantly from left to right, and also that there is significant leakage in the region outside the gaskets at left. This non-uniformity is even clearer in the cross-sectional view in Fig. 12. Fig. 13 represents a calibration of the flow NMR imaging and suggest an accuracy within about 10%.

Further investigation being reported elsewhere shows that macroscopically non-uniform flow is indeed responsible for the major skewness observed in Fig. 8, while much of the small-scale dispersion is concentrated in auxiliary equipment such as lines and valves.

Comments on use of the plate concept in present chromatographic practice

The success of short columns such as the MemSep in fractionating protein mixtures is certainly not due to a large plate count: devices of this type normally exhibit less than 100 plates. It is largely a result of gradient elution techniques in which solutes tend to be mobilized in

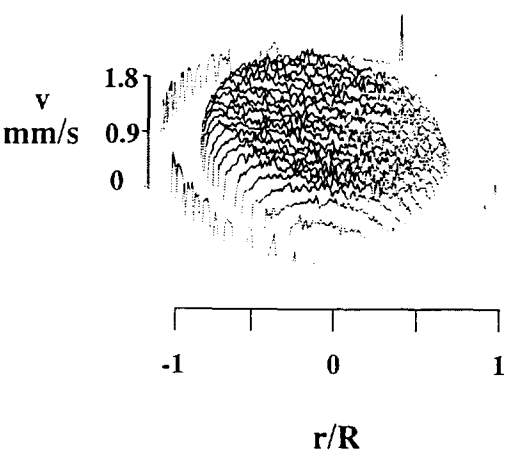

Fig. 11. Velocity distribution in a MemSep 1000. Shown is a velocity distribution over a 0.5-mm slice transverse to the axis and 10% of the distance from the stack inlet toward the outlet. The column I.D. is 25 mm and the water flow-rate is 13.5 mm/min. From Roper [32].

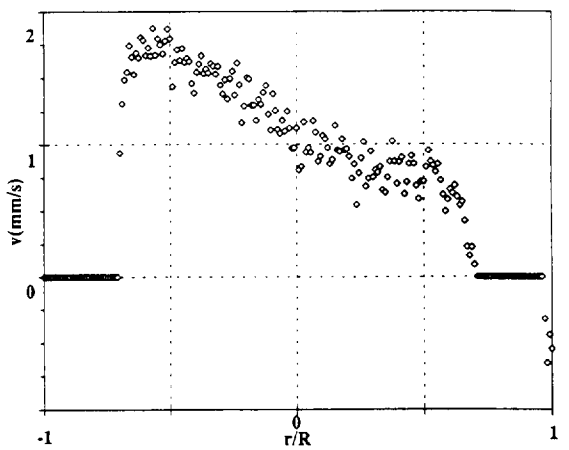

Fig. 12. Radial velocity distribution in a MemSep 1000. Shown is a radial trace of the velocity profile of Fig. 11. Slower velocities correspond to larger local residence times. From Roper [32].

sequence, a procedure popularly known as the "on–off" technique. In pure on–off behavior, high-quality separations can be achieved in a single mixing stage [4], and larger numbers of plates actually adversely affect the separation. However, it can be shown [4] that sensitivity to eluent concentration is seldom sufficient for pure on–off separation, certainly not under preparative conditions where reversed-phase columns tend to be damaging. Rather, one must depend on a judicious combination of the classical selective migration and what may be called differential elution produced by a properly chosen gradient elution program. Under these conditions the plate concept is of doubtful value, and numerical descriptions are almost always necessary. It is suggested here that the mass-transfer model is much preferable to the dispersion model under these circumstances.

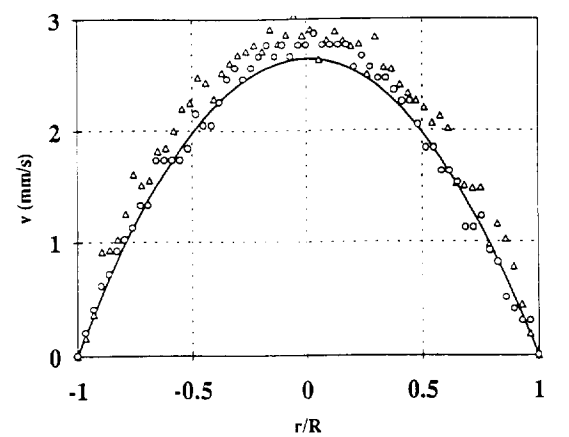

Fig. 13. Poiseuille flow in a tube by NMR flow imaging. Shown are velocity distributions measured to dynamic microscopy (○) and measurement of phase shifts (△) compared with predictions of Poiseuille flow (solid line). These comparisons suggest that the velocity data of the two previous figures are accurate to within less than 10% error. From Roper [32].

References

[1] A.M. Athalye, S.J. Gibbs and E.N. Lightfoot, J. Chromatogr., 589 (1992) 71.
[2] L.R. Snyder and M.A. Stadalius, High Performance Liquid Chromatography of Large Molecules, Vol. 4, 1986, p. 195.
[3] G. Cox, Chromatogr., 599 (1992) 195.
[4] J.L. Coffman, D.K. Roper, and E.N. Lightfoot, Bioseparation, 4 (1994) 183.
[5] D.K. Roper and E.N. Lightfoot, J. Chromatogr. A, 654 (1993) 1.
[6] D.K. Roper and E.N. Lightfoot, in Proceedings of PrepTech'94, Secaucus, NJ, March 22–24; 1994, in press.
[7] C.A. Brooks and S.M. Cramer, AIChE J, 38 (1992) 1969.
[8] N.B. Afeyan, N.F. Gordon, I. Mazsaroff, L. Varady, S.P. Fulton, Y.B. Yang and F.E. Regnier, J. Chromatogr., 519 (1990) 1.
[9] T.B. Tennikova, B.G. Belenkii and F. Svec, J. Liq. Chromatogr., 13 (1990) 63.
[10] J.A. Gerstner, R. Hamilton and S.M. Cramer, J. Chromatogr., 596 (1992) 173.
[11] A.J.P. Martin and R.L.M. Synge, Biochem. J., 35 (1941) 1359.
[12] J.J. van Deemter, F.J. Zuiderweg and A. Klinkenberg, Chem. Eng. Sci., 5 (1956) 271.
[13] P.J. Karol, Anal. Chem., 61 (1989) 1937.
[14] S.J. Gibbs and E.N. Lightfoot, Ind. Eng. Chem., Fundam., 25 (1986) 490.
[15] E. Glueckauf and J.I. Coates, J. Chem. Soc., (1947) 1315.
[16] A. Klinkenberg and F. Sjenitzer, Chem. Eng. Sci., 5 (1956) 258.
[17] J.F.G. Reis, E.N. Lightfoot, P.T. Noble and A.S. Chiang, Sep. Sci. Technol., 14 (1979) 367.
[18] E.N. Lightfoot, et al., in H.M. Schoen (Editor), New Chemical Engineering Separation Techniques, Interscience, New York, 1962.

[19] H.S. Carslaw and J.C. Jaeger, Conduction of Heat in Solids, Oxford University Press, Oxford, 2nd ed., 1959, Sect. 10.3.
[20] A. Anzelius, Z. Angew. Math. Mech., 6 (1926) 291.
[21] A.M. Lenhoff and E.N. Lightfoot, J. Theor. Biol., 106 (1984) 207.
[22] S.-Y. Suen and M.R. Etzel, Chem. Eng. Sci., 47 (1992) 1355.
[23] E.N. Lightfoot and E.J. Lightfoot, in Kirk-Othmer Encyclopedia of Chemical Technology, Wiley, New York, 4th ed., in press.
[24] Ross Taylor and R. Krishna, Multicomponent Mass Transfer, Wiley, New York, 1993.
[25] S.J. Gibbs and E.N. Lightfoot, Ind. Eng. Chem. Fundam., 25 (1986) 490.
[26] S.J. Gibbs, E.N. Lightfoot and T.W. Root, J. Phys. Chem., 96 (1992) 7458.
[27] J.L. Coffman, Doctoral Thesis, University of Wisconsin, Madison, WI, in preparation.
[28] N. Epstein, N., Chem. Eng. Sci., 44 (1989) 777.
[29] J.L. Anderson and J.A. Quinn, Biophys. J., 14 (1974) 130.
[30] A.M. Athalye, Doctoral Thesis, University of Wisconsin, Madison, WI, 1993.
[31] S. Yamamoto, et al., J. Chromatogr., 394 (1987) 363.
[32] D.K. Roper, Doctoral Thesis, University of Wisconsin, Madison, WI, 1994.
[33] S. Yamamoto, presented at Engineering Foundation Conference on Downstream Processing, Interlaken, Switzerland, September 1992.
[34] F. Balzereit, M.Sc. Thesis, University of Wisconsin, Madison, WI, 1991.
[35] K.R. Raths, Flow and Diffusion in Adsorptive Membrane Systems, M.Sc. Thesis, University of Wisconsin, Madison, WI, 1992.
[36] M.S. Jeansomme and J.-P. Foley, J. Chromatogr., 594 (1992) 1.